Research Article
Open Access

MJ Cell Press

MJ Mathematics and Computer Science

Available at:

https://mjcellpress.com/article/mjmcs02/

MJ - MATHEMATICS AND COMPUTER SCIENCE

Mathematical modeling of SARS-CoV-2 (COVID-19) pandemic in Cameroon accounting the role of boosted immune systems

Albert Kouchéré Guidzavaï[1], Joseph Yangla[2], Hamadjam Abboubakar[3,4*], Gnodandi Kaakréo[2], Rubin Fandio[5], Irépran Damakoa[2].

[1] *University of Yaoundé 1, Faculty of Science, Department of Mathematics, P.O. Box 812, Yaoundé, Cameroon.*

[2] *University of Ngaoundéré, Faculty of Science, Department of Mathematics and Computer Science, P.O. Box 454, Ngaoundéré, Cameroon.*

[3] *University of Ngaoundéré, University Institute of Technology, Department of Computer Engineering, P.O. Box 455, Ngaoundéré, Cameroon.*

[4] *University of Ngaoundéré, School of Geology and Mining Engineering, Department of Applied Mathematics and Computer Science, P.O. Box 115, Meiganga, Cameroon.*

[5] *University of Yaoundé 1, Faculty of Science, Department of Physics, P.O. Box 812, Yaoundé, Cameroon..*

**Corresponding author:* *h.abboubakar@gmail.com*

Key words

COVID-19 pandemic,
Booster immunity,
Mathematical model,
Fractional-order derivative,
Asymptotic stability,
Sensitivity analysis.

Abstract

This study proposes and analyzes a mathematical model for the transmission dynamics of COVID-19, explicitly accounting for the ability of the immune system in some individuals to eliminate the virus before they become infectious. A compartmental *Susceptible–Exposed–Asymptomatic–Symptomatic–Hospitalized–Recovered* (SEAIHR) model is formulated using both classical integer-order derivatives and Caputo fractional-order derivatives. The model is first examined by establishing the positivity and boundedness of solutions, followed by the computation of the basic reproduction number $\mathcal{R}_0$. The existence of equilibrium points is proven, and the asymptotic stability of the disease-free equilibrium is analyzed when $\mathcal{R}_0 < 1$. Epidemiological data from Cameroon are used to estimate model parameters and calibrate the system. Sensitivity analysis identifies the most influential parameters governing disease transmission. Numerical results indicate that $\mathcal{R}_0 \approx 1.6483$, suggesting that COVID-19 remains endemic despite declining mortality. Simulations further show that enhanced immune responses may contribute to the relatively low morbidity observed in sub-Saharan Africa.

Received: 19.11.2025 Accepted: 19.12.2025 Published online: 14.01.2026

How to cite this article: Kouchéré Guidzavaï, A., Yangla, J., Abboubakar, H., Kaakréo, G., Fandio, R., & Damakoa, I (2026). *Mathematical modeling of SARS-CoV-2 (COVID-19) 2 pandemic in Cameroon accounting the role of boosted immune systems.* **MJ Mathematics and Computer Science, 2**(1), 1-32. https://doi.org/10.63156/mjmcs02.

1 Introduction

Like any other infectious disease, COVID-19, or coronavirus disease 2019, is caused by the SARS-CoV-2 virus, which was first identified in Wuhan, China, in late 2019 [1, 2]. The SARS-CoV-2 virus subsequently spread worldwide at an exponential rate [3–6]. The first confirmed case of COVID-19 in Africa was reported in Egypt on 14 February 2020 and involved a foreign national who had recently traveled from China. Following this initial detection, several African countries began to report cases, most of which were linked to travelers returning from abroad. In the subsequent months, infections were documented in many African countries, including South Africa, Nigeria, Ghana, Senegal, and Cameroon [7, 8]. African governments implemented various measures to contain the spread of the virus, including quarantine policies, travel restrictions, public awareness campaigns, and limitations on public gatherings [9–11]. COVID-19 is transmitted mainly through respiratory droplets generated when people talk, cough, or sneeze, and it can also spread via contact with contaminated surfaces [12–15].

Clinical manifestations vary among individuals and may include fever, cough, fatigue, loss of taste or smell, body aches, and, in severe cases, respiratory distress or pneumonia. Most infected individuals experience mild symptoms; however, severe and complicated forms are more likely to develop in older adults and in patients with underlying health conditions [16–18]. Several preventive measures have therefore been implemented, including vaccination, mask wearing, social distancing, and frequent hand washing. To prevent infection and reduce disease severity, multiple vaccines have been developed and deployed worldwide [19–22]. The pandemic has had a profound global impact, leading to unprecedented social, economic, and health disruptions. Owing to the substantial resources devoted to combating the disease, many countries have observed a significant decline in incidence rates. Nevertheless, efforts to control the pandemic continue to evolve through vaccination campaigns and ongoing research into novel therapeutic strategies.

Research aimed at strengthening the immune system to combat COVID-19 remains crucial [23, 24]. Various approaches are currently under investigation, including vaccination, antiviral therapies, and lifestyle interventions such as diet and physical activity [24–26]. The objective is to enhance immune responsiveness so that the virus can be eliminated before becoming infectious. This field of research is dynamic and continuously evolving as new variants emerge and scientific understanding of immune mechanisms advances. Although vaccines represent a major tool in pandemic control, they are not sufficient on their own. Complementary strategies are therefore essential to ensure an effective and sustained immune response. A thorough understanding of immune responses to COVID-19 is fundamental to clarifying how the human body combats the disease. In this context, strengthening immunity through appropriate lifestyle choices may contribute to more effective disease control.

Mathematical modeling provides a powerful framework for characterizing infection dynamics and anticipating the emergence or decline of infectious diseases. Numerous studies have investigated disease transmission using

mathematical models [27–30]. Over the past five years, several useful mathematical models have been developed to analyze the COVID-19 pandemic and to design feasible strategies aimed at mitigating or even eliminating the infection [31–37].

The originality of our model compared with those developed in [31, 32] lies in the following aspects. In [32], the authors investigate the influence of nonpharmaceutical interventions on COVID-19 transmission. They consider both symptomatic and asymptomatic infected individuals but neglect susceptible individuals who are particularly vulnerable to the disease, such as hospitalized patients. In [33], the authors aim to describe the dynamics of COVID-19 in Turkey, formulating a classical model that is extended through the Atangana–Baleanu fractional derivative. In [38], a modified SIQR model is proposed to analyze the transmission dynamics of SARS-CoV-2 considering two variants, Delta and Omicron, and key parameters are identified through sensitivity analysis. In [34], the authors quantify the influence of nonpharmaceutical interventions (NPIs) on COVID-19 transmission rates in selected European regions, namely Spain and Italy, from February to December 2020, prior to the introduction of vaccination campaigns. Their objective is to examine correlations between NPI implementation, variations in transmission rates, and changes in life expectancy across different age and gender groups from 2019 to 2020. Their findings provide valuable insights into the effectiveness of NPIs in mitigating disease spread and contribute to a broader understanding of epidemic control strategies. In [35], the authors model COVID-19 dynamics by incorporating human behavioral responses and government interventions, and subsequently extend the model to include both zoonotic and human-to-human transmission. In [36], a novel mathematical model is proposed to assess the impact of hospitalization, quarantine measures, and pathogen load on controlling the COVID-19 pandemic. In [37], the authors draw inspiration from SEIR-type models by incorporating asymptomatic individuals, hospitalized patients, and particularly vulnerable populations at high risk, such as people living with HIV or asthma. These groups are more susceptible to COVID-19 infection than the general population, which constitutes a key originality of their work.

Our study is inspired by the existing literature and, more specifically, by [34, 36, 37]. We aim to model the transmission dynamics of COVID-19 by accounting for the fact that the immune system of certain individuals can clear the virus before it is transmitted to another susceptible person, thereby reducing secondary transmission. Following the formulation of the model using integer-order derivatives, we establish the non-negativity of the state variables, the boundedness of solutions, compute the basic reproduction number $\mathcal{R}_0$, and analyze the local and global stability of the disease-free equilibrium, as well as the existence of a unique endemic equilibrium when $\mathcal{R}_0 > 1$. Prior to introducing the fractional-order model, we review fundamental definitions and key results related to the Caputo derivative. We then demonstrate the existence and uniqueness of solutions to the fractional-order model. Using real COVID-19 data from Cameroon, the model is calibrated through parameter estimation and sensitivity analysis. Furthermore, we show mathematically that the fractional-order model provides a more

accurate representation of disease dynamics than the integer-order model. Finally, several numerical simulations are performed to validate the theoretical findings.

The manuscript is organized as follows: Section 2 is devoted to the formulation of the model using integer-order derivatives. In Section 3, we analyze the positivity and boundedness of solutions, compute the basic reproduction number, investigate the local and global asymptotic stability of the disease-free equilibrium, and establish the existence of a unique endemic equilibrium. Section 4 presents the fundamental definitions and useful results concerning fractional-order derivatives in the Caputo sense, together with proofs of existence and uniqueness of solutions. Section 5 focuses on model calibration and sensitivity analysis. Numerical simulations are provided in Section 6, and the paper concludes with a summary of the main findings.

2 Model formulation

Here, a compartmental mathematical model of the COVID-19 SEAIHR type is formulated. We divide the total population N into six compartments or classes: Susceptible S, Latent E, Asymptomatic A, Symptomatic I, Hospitalized H, and Recovered R; thus $N = S + E + A + I + H + R$. For better visualization, the compartmental structure is illustrated in Figure 1. According to the WHO, the virus can spread in two ways: human-to-human transmission and environmental transmission. The main mode of transmission of this disease occurs through respiratory droplets, direct contact, contaminated surfaces, and aerosols (in closed and poorly ventilated environments), and is characterized by a force of infection (FOI) given by

$$\lambda(t) = \beta_h \frac{A(t) + I(t)}{N(t) - \theta H(t)}, \tag{1}$$

where β_h represents the transmission rate, while θ denotes the proportion of hospitalized individuals who do not contribute to the dynamics of virus transmission. Note that $\theta = 0$ indicates that hospitalized individuals play a role equal to that of infectious individuals in transmission, whereas $\theta = 1$ implies that hospitalized individuals do not participate in transmission. Once individuals are infected, the virus spreads at a rate β_h, and they are classified as latent. Latent individuals may recover from the disease and become susceptible again at a rate c_1.

All the parameters of the model (2) are positive and are described in Table 1.

New individuals enter the susceptible population at the recruitment rate Λ through births, immigration, or emigration. After a latency period of duration $1/\gamma$, we assume that a fraction $(1 - c_1 - c_2)$ of latent individuals do not develop symptoms during the incubation period and become asymptomatic. However, the remaining proportion who exhibit clinical symptoms at the end of the incubation period develop symptoms at a progression rate c_2.

In our model, asymptomatic individuals may be admitted to hospital if they test positive, at a rate r_2.

Table 1: Description of model state variables and parameters.

Symbol	Description
S	Number of susceptible hosts
E	Number of latent hosts
A	Number of asymptomatic hosts
I	Number of symptomatic hosts
H	Number of hospitalized hosts
R	Number of recovered individuals
Λ	Recruitment rate
μ	Natural mortality rate
θ	Proportion of hospitalized individuals who receive treatment
β_h	Transmission rate
$1/\gamma$	Latency period
ξ	Proportion of recovered individuals who become susceptible again
δ_A	Additional mortality rate of asymptomatic individuals
δ_I	Additional mortality rate of symptomatic individuals
δ_H	Additional mortality rate of hospitalized individuals
c_1	Proportion of latent individuals in whom the immune system clears the virus before they become infectious
c_2	Proportion of latent individuals who become symptomatic
$1/\sigma_1$	Duration of the asymptomatic stage
$1/\sigma_2$	Duration of the symptomatic stage
σ_3	Recovery rate of hospitalized individuals
r_1	Proportion of asymptomatic individuals who become symptomatic
r_2	Proportion of asymptomatic individuals who become hospitalized
r_3	Proportion of symptomatic individuals who become asymptomatic
r_4	Proportion of symptomatic individuals who become hospitalized

Symptomatic individuals are also admitted to hospital at a rate r_4, and they may revert to the asymptomatic class at a rate r_3. Both asymptomatic and symptomatic individuals may recover at rates $(1 - r_1 - r_2)$ and $(1 - r_3 - r_4)$, respectively.

The fraction c_1 of latent individuals may become susceptible again as a result of their immune response. Recovered individuals may also return to the susceptible class after a certain period at a rate ξ.

Individuals in the asymptomatic, symptomatic, and hospitalized classes may die from the disease at rates δ_A, δ_I, and δ_H, respectively, in addition to the natural mortality rate μ that applies to all classes. The above description provides the epidemiological interpretation of the compartmental diagram in Figure 1.

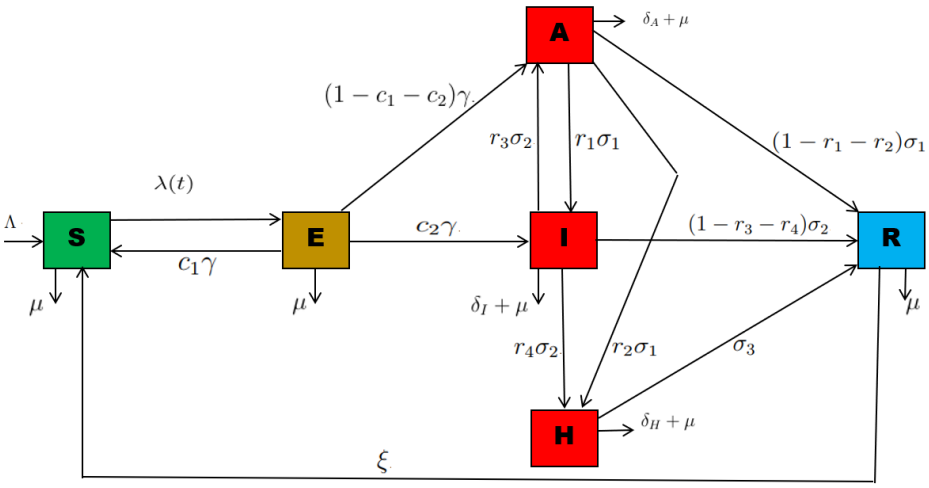

Figure 1: Compartmental representation of the transmission dynamics model for COVID-19.

Using the basic principles of compartmental modeling, the model described by Figure 1 is formulated as follows:

$$\begin{cases} \dot{S}(t) = \Lambda + c_1\gamma E(t) - \lambda(t)S(t) - \mu S(t) + \xi R(t), \\ \dot{E}(t) = \lambda(t)S(t) - (\mu + \gamma)E(t), \\ \dot{A}(t) = (1 - c_1 - c_2)\gamma E(t) + r_3\sigma_2 I(t) - (\sigma_1 + \delta_A + \mu)A(t), \\ \dot{I}(t) = c_2\gamma E(t) + r_1\sigma_1 A(t) - (\sigma_2 + \delta_I + \mu)I(t), \\ \dot{H}(t) = r_2\sigma_1 A(t) + r_4\sigma_2 I(t) - (\sigma_3 + \delta_H + \mu)H(t), \\ \dot{R}(t) = (1 - r_1 - r_2)\sigma_1 A(t) + (1 - r_3 - r_4)\sigma_2 I(t) + \sigma_3 H(t) - (\mu + \xi)R(t), \end{cases} \tag{2}$$

with initial conditions:

$$\begin{cases} S(0) = S_0 > 0, \quad E(0) = E_0 \geq 0, \quad A(0) = A_0 \geq 0, \quad I(0) = I_0 \geq 0, \\ H(0) = H_0 \geq 0, \quad R(0) = R_0 \geq 0. \end{cases} \tag{3}$$

Let $k_1 = \mu + \gamma$, $k_2 = \sigma_1 + \delta_A + \mu$, $k_3 = \sigma_2 + \delta_I + \mu$, $k_4 = \sigma_3 + \delta_H + \mu$, and $k_5 = \mu + \xi$. Then, the model can be rewritten as

$$\begin{aligned} \dot{S}(t) &= \Lambda + c_1\gamma E(t) - \lambda(t)S(t) - \mu S(t) + \xi R(t), \\ \dot{E}(t) &= \lambda(t)S(t) - k_1 E(t), \\ \dot{A}(t) &= (1 - c_1 - c_2)\gamma E(t) + r_3\sigma_2 I(t) - k_2 A(t), \\ \dot{I}(t) &= c_2\gamma E(t) + r_1\sigma_1 A(t) - k_3 I(t), \\ \dot{H}(t) &= r_2\sigma_1 A(t) + r_4\sigma_2 I(t) - k_4 H(t), \\ \dot{R}(t) &= (1 - r_1 - r_2)\sigma_1 A(t) + (1 - r_3 - r_4)\sigma_2 I(t) + \sigma_3 H(t) - k_5 R(t). \end{aligned} \tag{4}$$

3 Mathematical analysis

3.1 Basic properties

Since we consider a human population, all model parameters are non-negative.

Lemma 1. *Let us consider the model* (2) *coupled with the initial conditions given by* (3). *Then, the solutions* $(S(t), E(t), A(t), I(t), H(t), R(t))$ *of* (2) *will remain non-negative for all time* $t > 0$.

Proof. From (2), we have

$$\begin{aligned}
\dot{S}(t)\Big|_{S=0,E,R\geq 0} &= \Lambda + c_1\gamma E(t) + \xi R(t) > 0,\\
\dot{E}(t)\Big|_{E=0,S,A,I,H,R\geq 0} &= \lambda(t)S(t) \geq 0,\\
\dot{A}(t)\Big|_{A=0,S,E,I,H,R\geq 0} &= (1-c_1-c_2)\gamma E(t) + r_3\sigma_2 I(t) \geq 0,\\
\dot{I}(t)\Big|_{I=0,S,E,A,H,R\geq 0} &= c_2\gamma E(t) + r_1\sigma_1 A(t) \geq 0,\\
\dot{H}(t)\Big|_{H=0,S,E,A,I,R\geq 0} &= r_2\sigma_1 A(t) + r_4\sigma_2 I(t) \geq 0,\\
\dot{R}(t)\Big|_{R=0,S,E,A,I,H\geq 0} &= (1-r_1-r_2)\sigma_1 A(t) + (1-r_3-r_4)\sigma_2 I(t) + \sigma_3 H(t) \geq 0.
\end{aligned}$$

So, the non-negativity of the state variables of system (2) is ensured by the Barrier theorem [39]. This implies that $\mathbb{R}^6_+$ is an invariant set for the system (2). □

Lemma 2. *Let* $\mathcal{X} = (S, E, A, I, H, R) \in \mathbb{R}^6_+$. *The set* $C = \left\{ \mathcal{X} \in \mathbb{R}^6_+ : \sum_{i=1}^{6} \mathcal{X}_i \leq \frac{\Lambda}{\mu} \right\}$ *is positively invariant.*

Proof. Denote by $N(t)$ the total population, where $N(t) = S(t) + E(t) + A(t) + I(t) + H(t) + R(t)$.
Adding all equations of system (2) yields:

$$\begin{aligned}
\dot{N}(t) &= \Lambda - \mu N(t) - (\delta_A A(t) + \delta_I I(t) + \delta_H H(t)),\\
&\leq \Lambda - \mu N(t).
\end{aligned}$$

By integrating both sides of the above inequality and using the theory of differential inequalities, we obtain

$$0 < N(t) \leq N(0)e^{-\mu t} + \frac{\Lambda}{\mu}(1 - e^{-\mu t}). \tag{5}$$

When $t \to \infty$, we have $0 < N \leq \frac{\Lambda}{\mu}$. If $N(0) \leq \frac{\Lambda}{\mu}$ then $N(t) \leq \frac{\Lambda}{\mu}$. Thus, the set C is positively invariant, that is, all solutions with initial conditions in C remain in C for all $t > 0$. □

3.2 The basic reproduction number

We use the next-generation method to compute the basic reproduction number, denoted by $\mathcal{R}_0 = \rho(FV^{-1})$, where ρ is the spectral radius, F is the matrix of new infection terms, and V is the matrix of transition terms [40, 41]. The disease-free equilibrium (DFE) of the model is given by $E_0 = (S^*, E^*, A^*, I^*, H^*, R^*) = \left(\frac{\Lambda}{\mu}, 0, 0, 0, 0, 0\right)$. Let us set $y = (E, A, I, H)'$. The vectors $\mathcal{F}$ and $\mathcal{V}$, corresponding to the new infection terms and the remaining transfer terms for y, are respectively given by:

$$\mathcal{F} = \begin{pmatrix} \lambda(t)S(t) \\ 0 \\ 0 \\ 0 \end{pmatrix} \quad \text{and} \quad \mathcal{V} = \begin{pmatrix} -k_1 E \\ (1-c_1-c_2)\gamma E - k_2 A + r_3\sigma_2 I \\ c_2\gamma E + r_1\sigma_1 A - k_3 I \\ r_2\sigma_1 A + r_4\sigma_2 I - k_4 H \end{pmatrix}.$$

Their Jacobian matrices evaluated at E_0 are, respectively, given by

$$F = \begin{pmatrix} 0 & \beta_h & \beta_h & 0 \\ 0 & 0 & 0 & 0 \\ 0 & 0 & 0 & 0 \\ 0 & 0 & 0 & 0 \end{pmatrix} \quad \text{and} \quad V = \begin{pmatrix} -k_1 & 0 & 0 & 0 \\ (1-c_1-c_2)\gamma & -k_2 & r_3\sigma_2 & 0 \\ c_2\gamma & r_1\sigma_1 & -k_3 & 0 \\ 0 & r_2\sigma_1 & r_4\sigma_2 & -k_4 \end{pmatrix}. \tag{6}$$

The next-generation matrix (NGM), as described in [41], is $NGM = -FV^{-1}$. The basic reproduction number $\mathcal{R}_0$ is the spectral radius of NGM, that is, $\mathcal{R}_0 = \rho(-FV^{-1})$ [41]. By carrying out some calculations, we obtain:

$$\mathcal{R}_0 = \frac{(c_2\sigma_2 r_3 + (1-c_2-c_1)(k_3+\sigma_1 r_1) + c_2 k_2)\beta_h\gamma}{(k_2k_3 - r_1\sigma_1\sigma_2 r_3)k_1}. \tag{7}$$

The following result is a direct consequence of Theorem 2 in [41].

Lemma 3. *E_0 is locally asymptotically stable in C whenever $\mathcal{R}_0 < 1$, and unstable otherwise.*

3.3 Equilibrium points and stability analysis

Expressing each state variable of the model in terms of λ^* at equilibrium yields

$$\begin{aligned} S^* &= \frac{\Lambda + c_1\gamma E^* + \chi R^*}{\lambda^* + \mu}, \quad E^* = \frac{\lambda^*\,(R^*\xi + \Lambda)}{k_1\mu + \lambda^*\,(\mu + \gamma(1-c_1))}, \\ A^* &= \frac{(1-c_1-c_2)\gamma E^* + r_3\sigma_2 I^*}{k_2}, \quad I^* = \frac{c_2\gamma E^* + r_1\sigma_1}{k_3}, \\ H^* &= \frac{r_2\sigma_1 A^* + r_4\sigma_2 I^*}{k_4}, \quad R^* = \frac{(1-r_1-r_2)\sigma_1 A^* + (1-r_3-r_4)\sigma_2 I^* + \sigma_3 H^*}{k_5}. \end{aligned}$$

where λ^* is a non-negative solution of the following equation:

$$f(\lambda^*) = \lambda^* \left(a_2\lambda^* + a_1\right) = 0, \tag{8}$$

with

$$\begin{aligned} a_2 = &\left(\left(r_1\sigma_1\sigma_2\sigma_3 r_4 + \left(a_1\sigma_1 k_3 + r_1\sigma_1 a_2\sigma_2\right) k_4 + \sigma_1 r_2 k_3\sigma_3\right) c + c_2 k_2\sigma_2\sigma_3 r_4\right. \\ &+ \left(a_1\sigma_1 c_2\sigma_2 r_3 + a_2 c_2 k_2\sigma_2\right) k_4 + \sigma_1 c_2 r_2\sigma_2 r_3\sigma_3\Big)\gamma\xi \\ &+ \left(\left(r_1\sigma_1\sigma_2 r_4 + \sigma_1 r_2 k_3\right) k_5 c + \left(c_2 k_2\sigma_2 r_4 + \sigma_1 c_2 r_2\sigma_2 r_3\right) k_5\right)\gamma\theta\mu \\ &+ \left(\left(r_1\sigma_1 k_4 k_5 c + c_2 k_2 k_4 k_5\right)\delta_i + \left(\left(r_1\sigma_1\sigma_2 r_4 + \sigma_1 r_2 k_3\right) k_5 c + \left(c_2 k_2\sigma_2 r_4 + \sigma_1 c_2 r_2\sigma_2 r_3\right) k_5\right)\delta_h\right. \\ &\left.+ k_3 k_4 k_5\delta_a c + c_2\sigma_2 r_3 k_4 k_5\delta_a\right)\gamma + \left(k_2 k_3 - \sigma_1\sigma_2 r_1 r_3\right) k_4 k_5(c_1\gamma - k_1), \end{aligned}$$

and

$$a_1 = \left(\mathcal{R}_0 - 1\right) k_1 \left(k_2 k_3 - r_1\sigma_1\sigma_2 r_3\right) k_4 k_5\mu,$$

a_2 is always positive and $a_1 > 0 \Leftrightarrow \mathcal{R}_0 > 1$ (resp. $a_1 < 0 \Leftrightarrow \mathcal{R}_0 < 1$). Hence, model (2) admits a unique positive endemic equilibrium whenever $\mathcal{R}_0 > 1$, and no positive equilibrium otherwise. We summarize the above analysis as follows:

Theorem 1. *Model* (2) *admits, in addition to the disease-free equilibrium which always exists, an endemic equilibrium point that exists whenever* $\mathcal{R}_0 > 1$.

We use Theorem 2.1 in [42] to establish the global asymptotic stability of the COVID-free equilibrium using the same approach. Let $\mathcal{W} = (S, E, A, I, H, R)^t$ and $\mathcal{K} = (E, A, I, H)^t$. We consider system (2):

$$\dot{\mathcal{K}} = (F + V)\mathcal{K} - g(\mathcal{W}), \tag{9}$$

where F and V are given in (6) and

$$g(\mathcal{W}) = \begin{pmatrix} \beta_h(A + I)\left(1 - \dfrac{1}{N - \theta H}\right) \\ 0 \\ 0 \\ 0 \end{pmatrix} \geq \mathbf{0}_{\mathbb{R}^4}. \tag{10}$$

Using the results of Theorem 2.1 [42] and Theorem 3 [43], the condition for the global asymptotic stability of the COVID-free equilibrium is satisfied since $1 - \frac{1}{N-\theta H} \geq 0$ ensures that $g(\mathcal{W}) \geq \mathbf{O}_{\mathbb{R}^4}$. Consequently, we have

$\dot{\mathcal{K}} \leq (F+V)\mathcal{K}$. Moreover, the eigenvalues of $F+V$ have non-positive real parts, which implies that E_0 is locally stable when $\mathcal{R}_0 < 1$. Hence, $\mathcal{K} \to \mathbf{O}_{\mathbb{R}^4}$ as $t \to \infty$. In addition, we note that $F \geq \mathbf{O}_{\mathbb{R}^{4\times4}}$ and$-V^{-1} > \mathrm{O}_{\mathbb{R}^{4\times4}}$.

Inspired by Theorem 2.1 in [42], we introduce a Lyapunov function $\mathcal{P} = \mathcal{Z}(-V^{-1})\mathcal{W}$, where $\mathcal{Z}$ denotes the left eigenvector of $-FV^{-1}$ associated with the eigenvalue $\mathcal{R}_0$. Then, $\dot{\mathcal{P}} = (\mathcal{R}_0 - 1)\mathcal{Z}\mathcal{K} - \mathcal{Z}(-V^{-1})g(\mathcal{W}) \leq 0$. Therefore, the largest invariant set contained in $\left\{E \in \mathbb{R}^6 : \dot{\mathcal{P}} = 0\right\}$ is $\{E_0\}$. By applying LaSalle's invariance principle [44], we conclude that E_0 is globally asymptotically stable. Thus, we obtain the following result:

Theorem 2. *The disease-free equilibrium of the model* (2), $E_0 = \left(\frac{\Lambda}{\mu}, 0, 0, 0, 0, 0\right)$, *is globally asymptotically stable whenever* $\mathcal{R}_0 < 1$.

4 Fractional-order model in the Caputo sense

4.1 Basic concepts of fractional order

Since fractional-order derivatives are employed in this work, we briefly recall the main definitions and results related to fractional calculus.

Definition 1 ([45, 46]). *Let* $\mathbf{f} \in L^1([0;c], \mathbb{R}_+)$, $c > 0$. *The Riemann–Liouville fractional-order integral of* $\mathbf{f}$ *of order* $\varepsilon > 0$ *is defined as:*

$$ {}_c^C\mathcal{I}_t^{\varepsilon}\left(\mathbf{f}(t)\right) = \left(\Gamma(\varepsilon)\right)^{-1} \int_0^t \mathbf{f}(\theta)(t-\theta)^{\varepsilon-1} d\theta. \tag{11}$$

Definition 2 ([47]). *Let* $f \in \mathcal{C}^{\mathcal{L}}([0;c])$, $c > 0$, $\varepsilon \in \mathbb{R}$, *and* $\mathcal{L} \in \mathbb{N}$ *such that* $\mathcal{L} - 1 < \varepsilon < \mathcal{L}$. *The Caputo fractional-order derivative of* f *is defined by*

$$ {}_0^C D_t^{\varepsilon}\left(f(t)\right) = \frac{1}{\Gamma(\mathcal{L}-\varepsilon)} \int_0^t (t-\theta)^{\mathcal{L}-\varepsilon-1} f^{(\mathcal{L})}(\theta)\, d\theta, \quad t > 0. \tag{12}$$

Lemma 4 ([48]). *Let* $n = \lfloor \varepsilon \rfloor + 1$ *and* $\varepsilon \geq 0$. *Then,*

$$ {}_a^C\mathcal{I}_t^{\varepsilon}\left({}_a^C\mathcal{D}_t^{\varepsilon} f(t)\right) = f(t) - \sum_{k=0}^{n-1} \frac{f^k(0)}{k!} t^k. $$

If $0 < \varepsilon \leq 1$, *then*

$$ {}_a^C\mathcal{I}_t^{\varepsilon}\left(f(t)\right) = f(t) - f_0. $$

Lemma 5 ([46]). *Let* $\mathbf{f}(t) \in \mathcal{C}([a,b])$ *and* ${}_a^C D_t^{\varepsilon}\left(\mathbf{f}(t)\right) \in \mathcal{C}((a,b])$. *For* $0 < \varepsilon \leq 1$, *we have*

$$ \mathbf{f}(t) = \mathbf{f}(a) + \left(\Gamma(\varepsilon)\right)^{-1} \left({}_a^C D_t^{\varepsilon}\mathbf{f}\right)(\varsigma)(t-a)^{\varepsilon}, \qquad a \leq \varsigma \leq t, \qquad \forall t \in (a,b]. $$

Theorem 3 ([49]). *Consider the following fractional-order system in the Caputo sense:*

$$\begin{cases} {}_0^C D_t^{\varepsilon} \mathbf{x}(t) = \mathbf{f}(t, \mathbf{x}(t)), \\ \mathbf{x}(t_0) = \mathbf{x}_0, \end{cases}$$

with $0 < \varepsilon \leq 1$, *where* $\mathbf{f}$ *is a vector field. The equilibrium points of this system are locally asymptotically stable if the condition* $|\omega_i| > \varepsilon \dfrac{\pi}{2}$ *is satisfied, where* ω_i *denotes the eigenvalues of the Jacobian matrix of* $\mathbf{f}$ *evaluated at the equilibrium points and* $\varepsilon \in [0, 1)$.

Applying Definition 2 to the COVID-19 model (4) leads to the following fractional-order system:

$$\begin{cases} \chi^{\varepsilon-1} \times^C D_t^{\varepsilon} S(t) = \Lambda + c_1 \gamma E(t) - \lambda(t) S(t) - \mu S(t) + \xi R(t), \\ \chi^{\varepsilon-1} \times_0^C D_t^{\varepsilon} E(t) = \lambda(t) S(t) - k_1 E(t), \\ \chi^{\varepsilon-1} \times_0^C D_t^{\varepsilon} A(t) = (1 - c_1 - c_2)\gamma E(t) + r_3 \sigma_2 I(t) - k_2 A(t), \\ \chi^{\varepsilon-1} \times_0^C D_t^{\varepsilon} I(t) = c_2 \gamma E(t) + r_1 \sigma_1 A(t) - k_3 I(t), \\ \chi^{\varepsilon-1} \times_0^C D_t^{\varepsilon} H(t) = r_2 \sigma_1 A(t) + r_4 \sigma_2 I(t) - k_4 H(t), \\ \chi^{\varepsilon-1} \times_0^C D_t^{\varepsilon} R(t) = (1 - r_1 - r_2)\sigma_1 A(t) + (1 - r_3 - r_4)\sigma_2 I(t) + \sigma_3 H(t) - k_5 R(t), \end{cases} \tag{13}$$

where χ is introduced to ensure dimensional consistency [50–52]. The corresponding initial conditions are given by:

$$\begin{aligned} &S(0) = S_0 > 0, \quad E(0) = E_0 \geq 0, \quad A(0) = A_0 \geq 0, \\ &I(0) = I_0 \geq 0, \quad H(0) = H_0 \geq 0, \quad R(0) = R_0 \geq 0. \end{aligned} \tag{14}$$

4.2 Existence and uniqueness of solutions

This component of the paper demonstrates the existence and uniqueness of solutions to our fractional model. Let $\mathcal{X} = (S, E, A, I, H, R)$, and X be a Banach space of continuous functions with a real value defined on an interval χ with the related norm:

$$\|\mathcal{X}\| = \sum_{i=1}^{6} \|\mathcal{X}_i\|,$$

where $\|\mathcal{X}_i\| = \sup\{|\mathcal{X}_i(t)|, t \in \chi\}$, and $X = C(\mathcal{X}) \times C(\mathcal{X}) \times C(\mathcal{X}) \times C(\mathcal{X}) \times C(\mathcal{X}) \times C(\mathcal{X})$, with $C(\mathcal{X})$ is the Banach space of the continuous function of real value on $\mathcal{X}$ with the corresponding sup norm.

The model (13) can be rewrite as:

$$\begin{cases} {}^{C}D_t^{\varepsilon} S(t) = G_1(t, \mathcal{X}(t)), \\ {}^{C}D_t^{\varepsilon} E(t) = G_2(t, \mathcal{X}(t)), \\ {}^{C}D_t^{\varepsilon} A(t) = G_3(t, \mathcal{X}(t)), \\ {}^{C}D_t^{\varepsilon} I(t) = G_4(t, \mathcal{X}(t)), \\ {}^{C}D_t^{\varepsilon} H(t) = G_5(t, \mathcal{X}(t)), \\ {}^{C}D_t^{\varepsilon} R(t) = G_6(t, \mathcal{X}(t)). \end{cases} \tag{15}$$

In what foolows, we suppose that S, E, A, I, H, R are bounded, this means that there exists, κ_i, $i = 1, 2, \ldots, 9$ such that $\|\mathcal{X}_i\|_X \leq \kappa_i$.

Theorem 4. *Setting* $\mathcal{X}_1 = (S_1, E_1, A_1, I_1, H_1, R_1)$, $\mathcal{X}_2 = (S_2, E_2, A_2, I_2, H_2, R_2)$, *and* $\mathcal{G} = (G_1, G_2, G_3, G_4, G_5, G_6)$. *Then, there exists* $\mathcal{Q}_{\mathcal{G}}$ *such that:*

$$\|\mathcal{G}(t, \mathcal{X}_1(t)) - \mathcal{G}(t, \mathcal{X}_2(t))\|_X \leq \mathcal{Q}_{\mathcal{G}} \|\mathcal{X}_1(t) - \mathcal{X}_2(t)\|_X . \tag{16}$$

Proof. Let us prove that the kernels G_i for $i \in \{1, 2, 3, 4, 5, 6\}$ fulfill the Lipschitz condition. From (13), we have

$$\begin{aligned} \|G_1(t, S_1) - G_1(t, S_2)\| &= \|c_1\gamma(E_1 - E_2) - \mu(S_1 - S_2) + \xi(R_1 - R_2) - \lambda_1 S_1 + \lambda_2 S_2\| \\ &\leq c_1\gamma \|E_1 - E_2\| + \mu \|S_1 - S_2\| + \xi \|R_1 - R_2\| + \|\lambda_1 S_1 - \lambda_2 S_2\| \end{aligned} \tag{17}$$

where

$$\begin{aligned} \|\lambda_1 S_1 - \lambda_2 S_2\| &= \beta_h \left\| \frac{A_1 S_1 + I_1 S_1}{N_1 + (1-\theta)H_1} - \frac{A_2 S_2 + I_2 S_2}{N_2 + (1-\theta)H_2} \right\| \\ &\leq \frac{\beta_h}{\|(N_1 + (1-\theta)H_1)(N_2 + (1-\theta)H_2)\|} \|p_1 + p_2\| \end{aligned}$$

with $N_i = S_i + E_i + A_i + I_i + R_i$, for $i = 1, 2$, $p_1 = A_1 S_1(N_2 + (1-\theta)H_2) - A_2 S_2(N_1 + (1-\theta)H_1)$, and $p_2 = I_1 S_1(N_2 + (1-\theta)H_2) - I_2 S_2(N_1 + (1-\theta)H_1)$. The expression of p_1 is:

$$\begin{aligned} p_1 &= A_1 S_1(N_2 + (1-\theta)H_2) - A_2 S_2(N_1 + (1-\theta)H_1) \\ &= (A_1 S_1 N_2 - A_2 S_2 N_1) + (A_1 S_1(1-\theta)H_2 - A_2 S_2(1-\theta)H_1) \end{aligned}$$

where

$$
\begin{aligned}
A_1S_1N_2 - A_2S_2N_1 &= S_1S_2(A_1 - A_2) + A_1A_2(S_1 - S_2) + (A_1S_1E_2 - A_2S_2E_1) \\
&\quad + (A_1S_1I_2 - A_2S_2I_1) + (A_1S_1R_2 - A_2S_2R_1), \\
A_1S_1E_2 - A_2S_2E_1 &= \frac{1}{2}\left((A_1S_1 - A_2S_2)(E_2 - E_1)\right) + \frac{1}{2}\left((A_1S_1 + A_2S_2)(E_2 - E_1)\right) \\
&= -\frac{1}{2}(E_2 - E_1)\left(A_1S_1 - A_2S_2 + A_1S_1 + A_2S_2\right), \\
A_1S_1 - A_2S_2 &= \frac{1}{2}\left((S_1 - S_2)(A_1 - A_2) + (S_1 + S_2)(A_1 - A_2)\right) \\
&= \frac{1}{2}(A_1 - A_2)\left((S_1 - S_2) + (S_1 + S_2)\right), \\
A_1S_1E_2 - A_2S_2E_1 &= -\frac{1}{2}(E_2 - E_1)\left((A_1 - A_2)\left((S_1 - S_2) + (S_1 + S_2)\right) + (A_1S_1 + A_2S_2)\right), \\
A_1S_1I_2 - A_2S_2I_1 &= -\frac{1}{2}(I_2 - I_1)\left((A_1 - A_2)\left((S_1 - S_2) + (S_1 + S_2)\right) + (A_1S_1 + A_2S_2)\right), \\
A_1S_1R_2 - A_2S_2R_1 &= -\frac{1}{2}(R_2 - R_1)\left((A_1 - A_2)\left((S_1 - S_2) + (S_1 + S_2)\right) + (A_1S_1 + A_2S_2)\right), \\
A_1A_2(S_1 - S_2) + S_1S_2(A_1 - A_2) &= -\frac{1}{2}\left(\frac{1}{2}(A_1 - A_2)\left[(S_1 - S_2) + (S_1 + S_2)\right] + (A_1S_1 + A_2S_2)\right) \\
&\quad \times \left((E_1 - E_2) + (I_1 - I_2) + (R_1 - R_2)\right), \\
A_1S_1N_2 - A_2S_2N_1 &= A_1A_2(S_1 - S_2) + g_1(E_1 - E_2) + S_1S_2(A_1 - A_2) \\
&\quad + g_1(I_1 - I_2) + g_1(R_1 - R_2),
\end{aligned}
$$

with $g_1 = -\frac{1}{2}\left((A_1 - A_2)\left[(S_1 - S_2) + (S_1 + S_2)\right] + (A_1S_1 + A_2S_2)\right)$. Also, we have

$$
\begin{aligned}
A_1S_1(1-\theta)H_2 - A_2S_2(1-\theta)H_1 &= (1-\theta)\left(A_1S_1H_2 - A_2S_2H_1\right) \\
&= (1-\theta)\frac{1}{2}\left[-(A_1S_1 - A_2S_2)(H_1 - H_2)\right] \\
&\quad - (1-\theta)\frac{1}{2}\left[(A_1S_1 + A_2S_2)(H_1 - H_2)\right] \\
&= -(1-\theta)\frac{1}{4}(H_1 - H_2)\left[(S_1 - S_2)(A_1 - A_2) + (S_1 + S_2)(A_1 - A_2)\right] \\
&\quad - (1-\theta)\frac{1}{2}(H_1 - H_2)\left[(A_1S_1 + A_2S_2)\right]
\end{aligned}
$$

So,

$$
\begin{aligned}
p_1 &= A_1A_2(S_1 - S_2) + g_1(E_1 - E_2) + S_1S_2(A_1 - A_2) + g_1(I_1 - I_2) + g_1(R_1 - R_2) \\
&\quad + \frac{1}{2}(1-\theta)(H_1 - H_2)\left\{-\frac{1}{2}\left[(S_1 - S_2)(A_1 - A_2) + (S_1 + S_2)(A_1 - A_2)\right] - (S_1A_1 - S_2A_2)\right\}
\end{aligned}
$$

After algebraic simplifications, we obtain:

$$
\begin{aligned}
p_1 &= (S_1 - S_2)\left\{A_1A_2 + \frac{1}{2}(1-\theta)(H_1 - H_2)\right\} + g_1(E_1 - E_2) \\
&\quad + S_1S_2(A_1 - A_2) + g_1(I_1 - I_2) + g_1(R_1 - R_2) - (1-\theta)(H_1 - H_2)S_1A_1
\end{aligned}
$$

Similarly to p_1, we have:

$$p_2 = (S_1 - S_2)\left\{I_1 I_2 + \frac{1}{2}(1-\theta)(H_1 - H_2)\right\} + g_2(E_1 - E_2)$$
$$+ S_1 S_2(I_1 - I_2) + g_2(A_1 - A_2) + g_2(R_1 - R_2) - (1-\theta)(H_1 - H_2)S_1 I_1,$$

with $g_2 = \frac{1}{2}\{2S_2(I_1 - I_2) + S_1 I_1 + S_2 I_2\}$. Setting $g_3 = A_1 A_2 + (1-\theta)(H_1 - H_2) + I_1 I_2$, we thus obtain

$$\begin{aligned}
\|\lambda_1 S_1 - \lambda_2 S_2\| &\leq \frac{\beta_h}{\|(N_1 + (1-\theta)H_1)(N_2 + (1-\theta)H_2)\|}\|P_1 + P_2\| \\
&\leq \frac{\beta_h}{\|(N_1 + (1-\theta)H_1)(N_2 + (1-\theta)H_2)\|} \times (\|(S_1 - S_2)g_3 + (E_1 - E_2)(g_1 + g_2) + (A_1 - A_2)(S_1 S_2 + g_2) \\
&\qquad + (I_1 - I_2)(S_1 S_2 + g_1) + (1-\theta)(H_1 - H_2)(-S_1 A_1 + S_1 I_1) + (R_1 - R_2)(g_1 + g_2)\|) \\
&\leq \frac{\beta_h}{\|(N_1 + (1-\theta)H_1)(N_2 + (1-\theta)H_2)\|} \times (\|g_3\|\,\|S_1 - S_2\| + \|g_1 + g_2\|\,\|E_1 - E_2\| + \|S_1 S_2 + g_2\|\,\|A_1 - A_2\| \\
&\qquad + \|S_1 S_2 + g_1\|\,\|I_1 - I_2\| + (1-\theta)\,\|S_1 A_1 + S_1 I_1\|\,\|H_1 - H_2\| + \|g_1 + g_2\|\,\|R_1 - R_2\|)
\end{aligned}$$

Finally, we obtain:

$$\begin{aligned}
\|G_1(t, S_1) - G_1(t, S_2)\| &\leq (\|g_3\| + \mu)\,\|S_1 - S_2\| + (c_1\gamma + \|g_1 + g_2\|)\,\|E_1 - E_2\| \\
&\quad + (S_1 S_2 + \|g_2\|)\,\|A_1 - A_2\| + (S_1 S_2 + \|g_1\|)\,\|I_1 - I_2\| \\
&\quad + (1-\theta)\,\|S_1 A_1 + S_1 I_1\|\,\|H_1 - H_2\| + (\xi + \|g_1 + g_2\|)\,\|R_1 - R_2\| \\
&\quad \leq \omega_1(\|S_1 - S_2\| + \|E_1 - E_2\| + \|A_1 - A_2\| + \|I_1 - I_2\| + \|H_1 - H_2\| + \|R_1 - R_2\|),
\end{aligned}$$

where

$$\omega_1 = \max\left\{\frac{\beta_h\{\|g_3\| + \mu; c_1\gamma + \|g_1 + g_2\|; S_1 S_2 + \|g_2\|; S_1 S_2 + \|g_1\|; (1-\theta)\,\|S_1 A_1 + S_1 I_1\|; \xi + \|g_1 + g_2\|\}}{\|(N_1 + (1-\theta)H_1)(N_2 + (1-\theta)H_2)\|}\right\}.$$

A similar demonstration permits to obtain for G_2:

$$\begin{aligned}
\|G_2(t, E_1) - G_2(t, E_2)\| &\leq (\|g_3\|)\,\|S_1 - S_2\| + (\mu + \gamma + \|g_1 + g_2\|)\,\|E_1 - E_2\| \\
&\quad + (S_1 S_2 + \|g_2\|)\,\|A_1 - A_2\| + (S_1 S_2 + \|g_1\|)\,\|I_1 - I_2\| \\
&\quad + (1-\theta)\,\|S_1 A_1 + S_1 I_1\|\,\|H_1 - H_2\| + (\|g_1 + g_2\|)\,\|R_1 - R_2\| \\
&\quad \leq \omega_2(\|S_1 - S_2\| + \|E_1 - E_2\| + \|A_1 - A_2\| + \|I_1 - I_2\| + \|H_1 - H_2\| \\
&\qquad + \|R_1 - R_2\|),
\end{aligned}$$

where

$$\omega_2 = \max\left\{\frac{\beta_h\{\|g_3\|, \mu + \gamma + \|g_1 + g_2\|, S_1 S_2 + \|g_2\|, S_1 S_2 + \|g_1\|, (1-\theta)\,\|S_1 A_1 + S_1 I_1\|, \|g_1 + g_2\|\}}{\|(N_1 + (1-\theta)H_1)(N_2 + (1-\theta)H_2)\|}\right\}.$$

With the same technique, we obtain:

$$\begin{aligned}
\|G_3(t,A_1)-G_3(t,A_2)\| &\leq (1-c_1-c_2)\gamma\|E_1-E_2\|+r_3\sigma_2\|I_1-I_2\|+k_2\|A_1-A_2\| \\
&\leq \omega_3\left(\|E_1-E_2\|+\|I_1-I_2\|+\|A_1-A_2\|\right), \\
\|G_4(t,I_1)-G_4(t,I_2)\| &\leq c_2\gamma\|E_1-E_2\|+r_1\sigma_1\|A_1-A_2\|+k_3\|I_1-I_2\| \\
&\leq \omega_4\left(\|E_1-E_2\|+\|I_1-I_2\|+\|A_1-A_2\|\right), \\
\|G_5(t,H_1)-G_5(t,H_2)\| &\leq r_2\sigma_1\|A_1-A_2\|+r_4\sigma_2\|I_1-I_2\|+k_4\|H_1-H_2\| \\
&\leq \omega_5\left(\|A_1-A_2\|+\|I_1-I_2\|+\|H_1-H_2\|\right), \\
\|G_6(t,R_1)-G_6(t,R_2)\| &\leq (1-r_1-r_2)\sigma_1\|A_1-A_2\|+(1-r_3-r_4)\sigma_2\|I_1-I_2\| \\
&\quad +\sigma_3\|H_1-H_2\|+k_5\|R_1-R_2\| \\
&\quad \omega_6\left(\|A_1-A_2\|+\|I_1-I_2\|+\|H_1-H_2\|+\|R_1-R_2\|\right),
\end{aligned} \tag{18}$$

where $\omega_3=\max\{(1-c_1-c_2)\gamma;r_3\sigma_2;k_2\}$, $\omega_4=\max\{c_2\gamma;r_1\sigma_1;k_3\}$, $\omega_5=\max\{r_2\sigma_1;r_4\sigma_2;k_4\}$, and $\omega_6=\max\{(1-r_1-r_2)\sigma_1;(1-r_3-r_4)\sigma_2;\sigma_3;k_5\}$.

Consequently,

$$\|\mathcal{G}(t,\mathcal{X}_1(t))-\mathcal{G}(t,\mathcal{X}_2(t))\|_X=\sup_{t\in[0;T_f]}\sum_{i=1}^{6}|G_i(t,\mathcal{X}_1(t))-G_i(t,\mathcal{X}_2(t))|\leq\mathcal{Q}_{\mathcal{G}}\|\mathcal{X}_1(t)-\mathcal{X}_2(t)\|_X, \tag{19}$$

where $\mathcal{Q}_{\mathcal{G}}=\sum_{i=1}^{6}\omega_i$. Since $\mathcal{G}:[0,t]\times\mathbb{R}_+^6\to\mathbb{R}_+^6$ is continuous, it follow from [53] that solutions of system (13) exist. □

Theorem 5. *Assume that Theorem 4 holds. If* $\frac{t_f}{\Gamma(\varepsilon+1)}\mathcal{Q}_{\mathcal{G}}<1$, *then system* (13) *admits a unique uniformly Lyapunov stable solution on* $[0,t_f]$.

Proof. Let us define: $\mathcal{B}:X\to X$ such that

$$(\mathcal{B}\mathcal{X})(t)=\mathcal{X}_0+\frac{1}{\Gamma(\varepsilon)}\int_0^t(t-\alpha)^{\varepsilon-1}\mathcal{G}(\alpha,\mathcal{X}(\alpha))d\alpha,$$

which is well defined since $\mathcal{Q}$ is continious. The integral form of equation (13) is given by:

$$\mathcal{X}(t)=\mathcal{X}_0+\frac{1}{\Gamma(\varepsilon)}\int_0^t(t-\alpha)^{\varepsilon-1}\mathcal{G}(\alpha,\mathcal{X}(\alpha))d\alpha.$$

For the uniqueness, we will show that $\mathcal{H}$ is both a self-application and a contraction. Note that $\sup_{t\in[0,t_f]}|\mathcal{G}(t,O)\|=\Lambda$.

Now, Let us define $\mathcal{L} > \dfrac{|\mathcal{X}_0\| + \left(\dfrac{t_f}{\Gamma(\varepsilon+1)}\right)\Lambda}{1-\left(\dfrac{t_f}{\Gamma(\varepsilon+1)}\right)\mathcal{Q}_{\mathcal{G}}}$ and $D_X = \{\mathcal{X} \in X : |\mathcal{X}_0\|_X \leq \mathcal{L}\}$. Let $\mathcal{X} \in D_X$, then

$$
\begin{aligned}
|\mathcal{B}\mathcal{X}\|_X &= \sup_{t\in[0,t_f]}\left\{\left|\mathcal{X}_0 + \frac{1}{\Gamma(\varepsilon)}\int_0^t (t-\alpha)^{\varepsilon-1}\mathcal{G}(\alpha,\mathcal{X}(\alpha))d\alpha\right|\right\} \\
&\leq |\mathcal{X}_0| + \frac{1}{\Gamma(\varepsilon)}\sup_{t\in[0,t_f]}\left\{\int_0^t (t-\alpha)^{\varepsilon-1}\left(|\mathcal{G}(\alpha,\mathcal{X}(\alpha)) - \mathcal{G}(\alpha,0)| + |\mathcal{G}(\alpha,0)|\right)d\alpha\right\} \\
&\leq |\mathcal{X}_0| + \frac{1}{\Gamma(\varepsilon)}\sup_{t\in[0,t_f]}\left\{\int_0^t (t-\alpha)^{\varepsilon-1}\left(\|\mathcal{G}(\alpha,\mathcal{X}(\alpha)) - \mathcal{G}(\alpha,0)\|_X + \|\mathcal{G}(\alpha,0)\|_X\right)d\alpha\right\} \\
&\leq |\mathcal{X}_0| + \frac{\mathcal{Q}_{\mathcal{G}}\|\mathcal{X}_X + \Lambda\|}{\Gamma(\varepsilon)}\sup_{t\in[0,t_f]}\left\{\int_0^t (t-\alpha)^{\varepsilon-1}d\alpha\right\} \\
&\leq |\mathcal{X}_0| + \frac{\mathcal{Q}_{\mathcal{G}}\mathcal{L}+\Lambda}{\Gamma(\varepsilon)}\sup_{t\in[0,t_f]}\left\{\int_0^t (t-\alpha)^{\varepsilon-1}d\alpha\right\} \\
&\leq |\mathcal{X}_0| + \frac{\mathcal{Q}_{\mathcal{G}}\mathcal{L}+\Lambda}{\Gamma(\varepsilon+1)}t_f \\
&\leq |\mathcal{X}_0| + \left(\frac{t_f}{\Gamma(\varepsilon+1)}\right)(\mathcal{Q}_{\mathcal{G}}+\Lambda) \\
&\leq \mathcal{L}.
\end{aligned}
$$

This prove that $\mathcal{B}D_X \subseteq D_X$, and thus $\mathcal{B}$ is a self-map. It remains to show that $\mathcal{B}$ is a contraction. Using Theorem 4, we have:

$$
\begin{aligned}
\|\mathcal{B}\mathcal{X}_1 - \mathcal{B}\mathcal{X}_2\|_X &= \sup_{t\in[0,t_f]}\{|\mathcal{B}\mathcal{X}_1 - \mathcal{B}\mathcal{X}_2|\}, \\
&= \frac{1}{\Gamma(\varepsilon)}\sup_{t\in[0,t_f]}\left\{\int_0^t (t-\alpha)^{\varepsilon-1}|\mathcal{G}(\alpha,\mathcal{X}_1(\alpha)) - \mathcal{G}(\alpha,\mathcal{X}_2(\alpha))|\,d\alpha\right\}, \\
&\leq \frac{\mathcal{Q}_{\mathcal{G}}}{\Gamma(\varepsilon)}\sup_{t\in[0,t_f]}\left\{\int_0^t (t-\alpha)^{\varepsilon-1}|\mathcal{X}_1(\alpha) - \mathcal{X}_2(\alpha)|\,d\alpha\right\}, \\
&\leq \left(\frac{t_f}{\Gamma(\varepsilon+1)}\right)\mathcal{Q}_{\mathcal{G}}\|\mathcal{X}_1(\alpha) - \mathcal{X}_2(\alpha)\|_X.
\end{aligned}
$$

Thus, $\mathcal{B}$ is a contraction if $\left(\dfrac{t_f}{\Gamma(\varepsilon+1)}\right)\mathcal{Q}_{\mathcal{G}} < 1$. By the Banach contraction principle, we conclude that $\mathcal{B}$ has a unique point on $[0, t_f]$ which is a solution of (13). The uniformly Lyapunov stability of the solution of (13) comes from [54]. □

4.3 The basic reproduction number of the fractional model and stability analysis of the DFE

Let us set $y = (E, A, I, H)'$. The vector $\mathcal{F}$ and $\mathcal{V}$ for the new infection terms and the remaining transfer terms for y are, respectively, given by:

$$\chi^{\varepsilon-1} \times \mathcal{F} = \begin{pmatrix} \lambda(t)S(t) \\ 0 \\ 0 \\ 0 \end{pmatrix} \quad \text{and} \quad \chi^{\varepsilon-1} \times \mathcal{V} = \begin{pmatrix} -k_1 E \\ (1-c_1-c_2)\gamma E - k_2 A + r_3\sigma_2 \\ c_2\gamma E + r_1\sigma_1 A - k_3 I \\ r_2\sigma_1 A(t) + r_4\sigma_2 I(t) - k_4 H(t) \end{pmatrix}.$$

Their Jacobian matrices evaluated at E_0 are, respectively, given by

$$\chi^{\varepsilon-1} \times F = \begin{pmatrix} 0 & \beta_h & \beta_h & 0 \\ 0 & 0 & 0 & 0 \\ 0 & 0 & 0 & 0 \\ 0 & 0 & 0 & 0 \end{pmatrix} \quad \text{and} \quad \chi^{\varepsilon-1} \times V = \begin{pmatrix} -k_1 & 0 & 0 & 0 \\ (1-c_1-c_2)\gamma & -k_2 & r_3\sigma_2 & 0 \\ c_2\gamma & r_1\sigma_1 & -k_3 & 0 \\ 0 & r_2\sigma_1 & r_4\sigma_2 & -k_4 \end{pmatrix}.$$

The next-generation matrix (NGM), as described in [41] is $NGM = -FV^{-1}$. The basic reproduction number $\mathcal{R}_0$ is the spectral radius of NGM. That is $\mathcal{R}_0 = \rho(-FV^{-1})$ [41]. By carrying out some calculations, we obtain:

$$\chi^{\varepsilon-1} \times \mathcal{R}_0 = \frac{(c_2\sigma_2 r_3 + (1-c_2-c_1)(k_3+\sigma_1 r_1) + c_2 k_2)\beta_h\gamma}{(k_2k_3 - r_1\sigma_1\sigma_2 r_3)k_1}, \tag{20}$$

where χ is used to balance the unit.

Using the useful Theorem 3, it follows that to demonstrate the local stability of the COVID-free equilibrium, it is necessary to show that all the eigenvalues of the Jacobian matrix of (13) evaluated in the COVID-free equilibrium have nonpositive real components.

Let J the Jacobian matrix of (13) evaluated at $E_0 = \left(\frac{\Lambda}{\mu}, 0, 0, 0, 0, 0\right)$. We have

$$J = \begin{pmatrix} -\mu & c_1\gamma & -\beta_h & -\beta_h & 0 & \xi \\ 0 & -k_1 & \beta_h & \beta_h & 0 & 0 \\ 0 & (1-c_1-c_2)\gamma & -k_2 & r_3\sigma_2 & 0 & 0 \\ 0 & c_2\gamma & r_1\sigma_1 & -k_3 & 0 & 0 \\ 0 & 0 & r_2\sigma_1 & r_4\sigma_2 & -k_4 & 0 \\ 0 & 0 & (1-r_1-r_2)\sigma_1 & (1-r_3-r_4)\sigma_2 & \sigma_3 & -k_5 \end{pmatrix}.$$

The eigenvalues of J are $-\mu$, $-k_5$ and those of the following sub-matrix

$$J_1 = \begin{pmatrix} -k_1 & \beta_h & \beta_h & 0 \\ c_3\gamma & -k_2 & r_3\sigma_2 & 0 \\ c_2\gamma & r_1\sigma_1 & -k_3 & 0 \\ 0 & r_2\sigma_1 & r_4\sigma_2 & -k_4 \end{pmatrix} = F - V,$$

where $c_3 = (1 - c_1 - c_2)$, F and V are given at Eq. (4.3). From Lemma 3 (consequence of [41, Theorem 2]), it follows that all eigenvalues of J_1 have a negative real part. Using Theorem 3, we conclude that the point E_0 is LAS. We thus claim the following result:

Lemma 6. *The disease-free equilibrium E_0 of the COVID-19 fractional-order model* (13) *is locally asymptotically stable whenever $\mathcal{R}_0 > 1$.*

Now, using [55, Corollary 2], it follows that the proof of the global stability of E_0 can be obtained using the same Lyapunov function used to prove the GAS of E_0 in the case of the integer model. Thus, we claim what follows:

Theorem 6. *The COVID-19 free equilibrium point of the fractional model is globally asymptotically stable whenever $R_0 < 1$, and unstable otherwise.*

5 Model calibration, forecasting and sensitivity analysis

5.1 Model calibration and forecasting

To obtain reliable predictions, it is essential to calibrate the model using actual data [56]. This process consists of comparing model outputs with field observations in order to identify points of convergence. In this study, we collected data on confirmed and cumulative COVID-19 cases in Cameroon. The country recorded its first case on 6 March 2020, and a cumulative total of 3000 cases was reported in May 2020 [56, 57].

For parameter estimation, we used the MATLAB function **lsqcurvefit**. In our context, model calibration amounts to solving the optimization problem

$$\min_{\Xi} \left\| I^{predict} - I^{data} \right\|,$$

where $\Xi = (\theta, \beta_h, \gamma, \ldots, r_4)$. The following initial conditions were adopted: $S(0) = 29{,}983{,}678$, $E(0) = 7891$, $A(0) = 7521$, $I(0) = 370$, $H(0) = 300$, and $R(0) = 240$. The results are presented in Figure 2 and Table 2. With these estimated parameter values, we obtain $\mathcal{R}_0 \approx 1.6483$, indicating that the disease remains endemic in the country. Figure 2 illustrates the cumulative number of confirmed cases, showing an approximately linear trend.

Table 2: Estimated values of model parameters and their source, with the corresponding estimated value of $\mathcal{R}_0$.

Parameter	Value	Source	Parameter	Value	Source
N_0	30×10^6	[58]	c_1	0.140734708376245	Estimated
μ	$\frac{1}{60 \times 12}$	[58]	c_2	0.000000022122400	Estimated
Λ	$N_0 \times \mu$	From 2	σ_1	0.320161490606443	Estimated
θ	0.026518463208512	Estimated	σ_2	0.017138639274454	Estimated
β_h	0.943299147493544	Estimated	σ_3	0.010925462901358	Estimated
γ	0.052619591865217	Estimated	r_1	0.000017976472485	Estimated
ξ	0.000564607767546	Estimated	r_2	0.194165646142496	Estimated
δ_A	0.157703635708349	Estimated	r_3	0.085317308143571	Estimated
δ_I	0.001034211160909	Estimated	r_4	0.009961138599839	Estimated
δ_H	0.001903012849783	Estimated	$\mathcal{R}_0$	1.648256802456525	Eq. (7)

In Figure 3, the red band provides a forecast of disease evolution up to March 2026, whereas the blue band represents the reported COVID-19 cases from March 2020 to March 2022. These predictions may assist decision makers, particularly government authorities, in implementing appropriate preventive strategies, such as barrier measures, vaccination, and social distancing, to better control the disease in the future.

Based on the epidemiological parameters estimated from the outbreak data shown in Figure 3, the model predicts that, in the absence of effective control measures and behavioral changes, a large proportion of the Cameroonian population could become infected by March 2026.

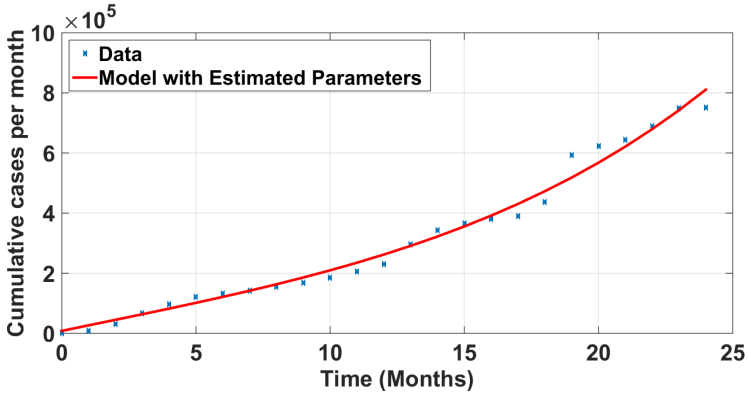

Figure 2: Cumulative real data per month (March 2020 - March 2022) versus model fitting.

In figure 3, the blue parts represent confirmed reported cases of COVID-19 during the period from March 2020 to March 2022, that is, 2 years and 1 month, while the red part represents a prediction of 36 months, that is, 3 years from April 2022 to April 2026 of COVID-19 in Cameroon.

“‘latex

5.2 Sensitivity analysis

Sensitivity analysis is a key factor in the choice of illness management. It provides a clear image of the sensitive and influential parameters of the model as well as their effect on the base reproduction rate. The sensitivity index

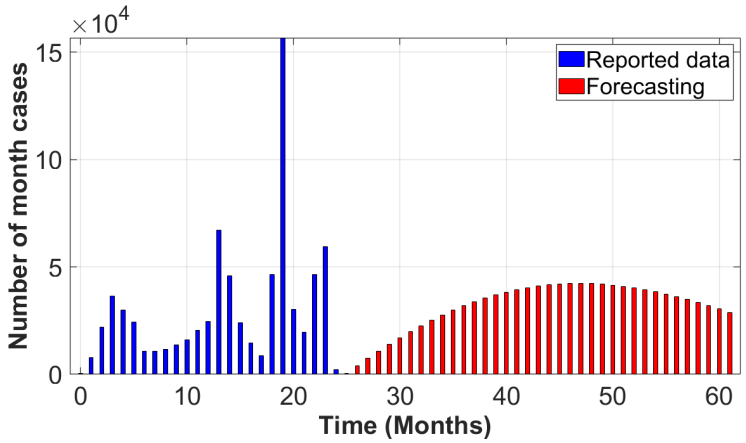

Figure 3: Confirmed Case and Disease Prediction: Period from March 2020 to March 2026. Prediction is from March 2022 to March 2026 and Confirmed Cases is from March 2020 to March 2022.

(see [59]) is calculated using the analytical expression $\mathcal{R}_0$ as follows:

$$\mathcal{N}_{p_i}^{\mathcal{R}_0} = \frac{\partial \mathcal{R}_0}{\partial p_i} \times \frac{p_i}{\mathcal{R}_0},$$

where p_i is a model parameter. Note that if p_i does not appear in the expression of $\mathcal{R}_0$, then $\mathcal{N}_{p_i}^{\mathcal{R}_0} = 0$. The sensitivity index of each model parameter is presented in Table 3 and Figure 4. Negative sensitivity indices indicate that increasing the value of the model parameter leads to a decrease in the value of $\mathcal{R}_0$, while positive indices indicate that increasing the value of the model parameter (respectively decreasing it) leads to an increase (respectively decreasing) in the value of $\mathcal{R}_0$ [59].

Table 3: Sensitivity indices of $\mathcal{R}_0$ for each model parameter.

Parameter	Sensitivity index	Parameter	Sensitivity index
β_h	1	δ_I	-0.1022
γ	0.6404	μ	-0.6960
c_2	0.3675	r_1	3.8986×10^{-6}
σ_2	-0.2970	σ_1	-0.0042
r_3	0.0223	δ_A	-0.3301
c_1	-0.2400	δ_H	0

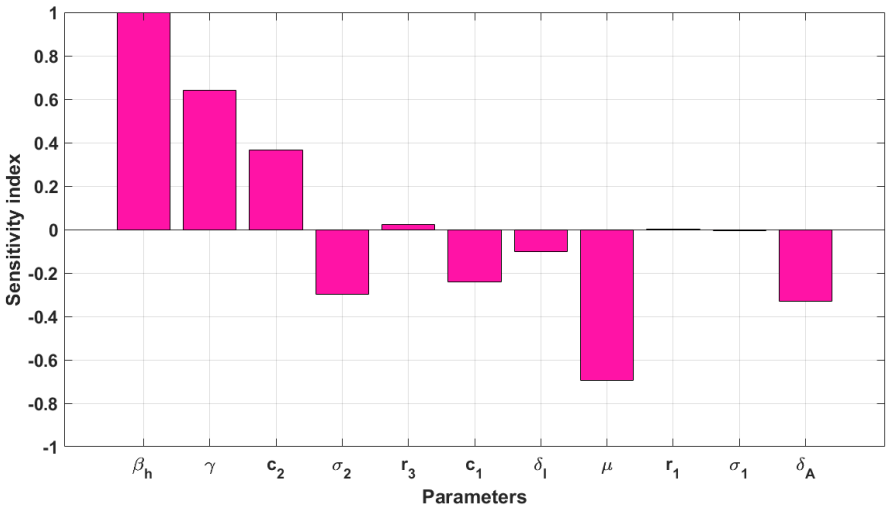

Figure 4: Sensitivity indices of $\mathcal{R}_0$ for each model parameter.

From Table 3 and Figure 4, it follows that the most sensitive parameter is β_h, followed by μ, γ, c_2, σ_2, and c_1. Increasing (resp. decreasing) β_h by 10% will result in an increase (resp. decrease) of the value of $\mathcal{R}_0$ by 10%. However, increasing the value of c_1 by 10% results in a decrease in the value of $\mathcal{R}_0$ by 2.4%.

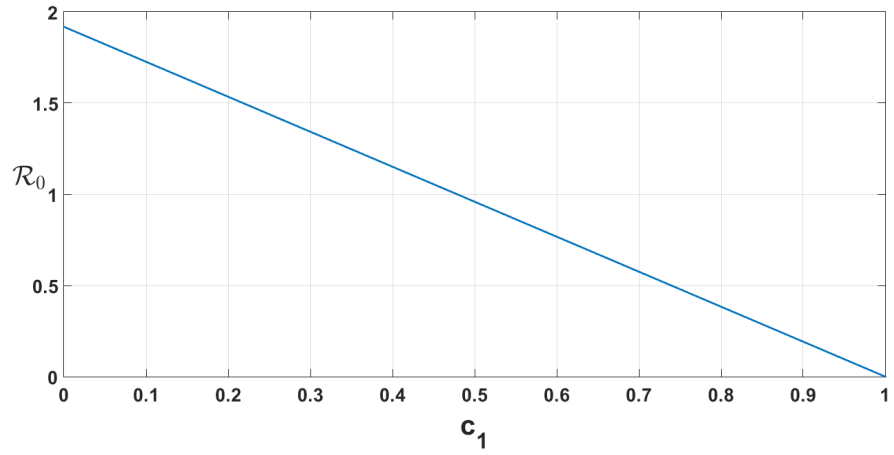

Figure 5: Behavior of $\mathcal{R}_0$ as a function of c_1.

In what follows, we present the different behavior of $\mathcal{R}_0$ as a function of some model parameters, which allows us to validate the results of the sensitivity analysis. In Figure 5, we have plotted the basic reproduction rate $\mathcal{R}_0$ as a function of c_1, the proportion of latent individuals who become susceptible due to increased immunity. We observe that as the proportion c_1 increases, the threshold $\mathcal{R}_0$ decreases. This decreasing behavior of $\mathcal{R}_0$ explains the fact that all drugs or natural products that allow the immune system to increase participate in the disease burden. On the other hand, when the contact rate β_h and the proportion c_2 of latent ones that will become asymptomatic increase, then the basic reproduction number $\mathcal{R}_0$ also increases (Figures 6, 7, and 8).

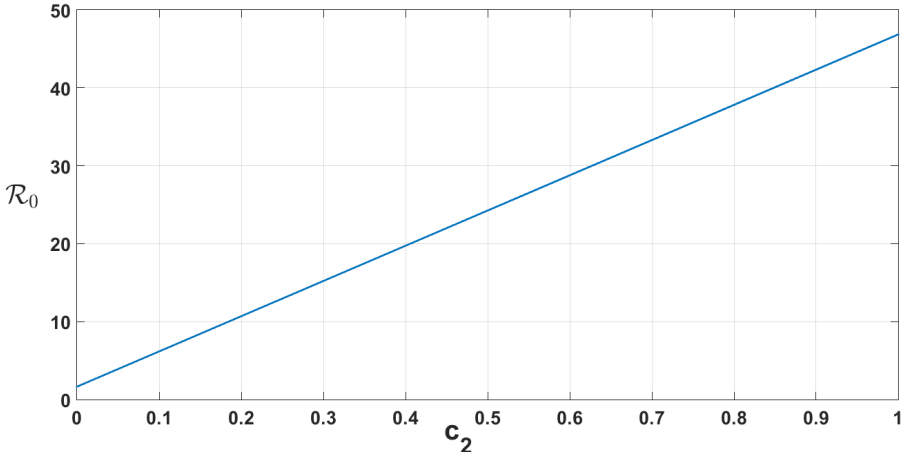

Figure 6: Behavior of $\mathcal{R}_0$ as a function of c_2.

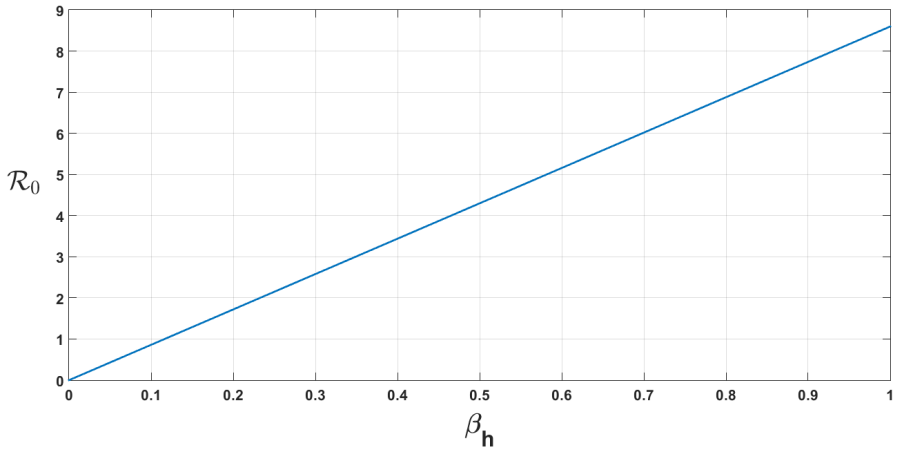

Figure 7: Behavior of $\mathcal{R}_0$ as a function of β_h.

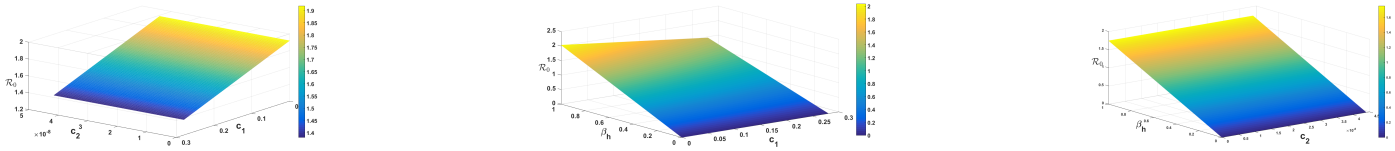

(a) c_1 and c_2 (b) c_1 and β_h (c) c_2 and β_h

Figure 8: 3-D behavior of $\mathcal{R}_0$ as a function of (a) c_1 and c_2, (b) c_1 and β_h, and (c) c_2 and β_h.

Figure 9 shows that the parameter c_1 (proportion of latent individuals in whom the immune system cleared the virus before they became infectious) plays a crucial role in the dynamics of the disease. Increasing c_1 allows to increase the number of susceptible persons and decrease the density of infected individuals. This confirms that the fight against COVID-19 involves reducing contact with infected people and improving the immune system.

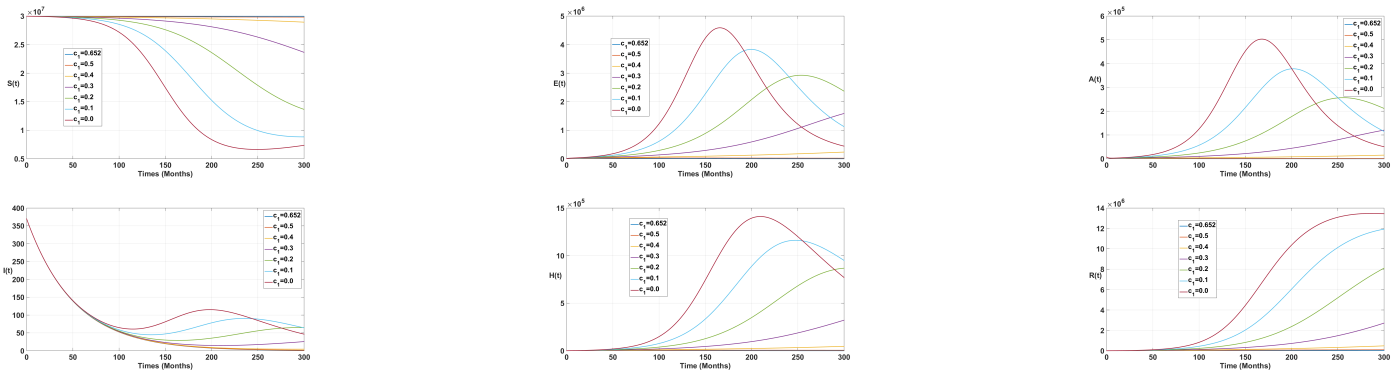

Figure 9: Time-series of model state variables as a function of the model parameter c_1.

5.3 Impact of the fractional operator

The impact of fractional derivative on the COVID-19 dynamics is depicted in Figure 10. In a quantitative point of view, according to Figure 4, it is clear that the model with fractional order derivatives is better suited than the one with ordinary derivatives. Indeed, the $RMSE_{\varepsilon=1} = 1.7973$ while the $RMSE_{\varepsilon=0.9} = 1.7882$, where $RMSE$ denotes the root-mean-square error is given by the following formula:

$$RMSE = \sqrt{\frac{\sum (I_i - I^i)^2}{n}} \tag{21}$$

where

- I_i represents observed values;
- I^i represents predicted values;
- n total number of observations.

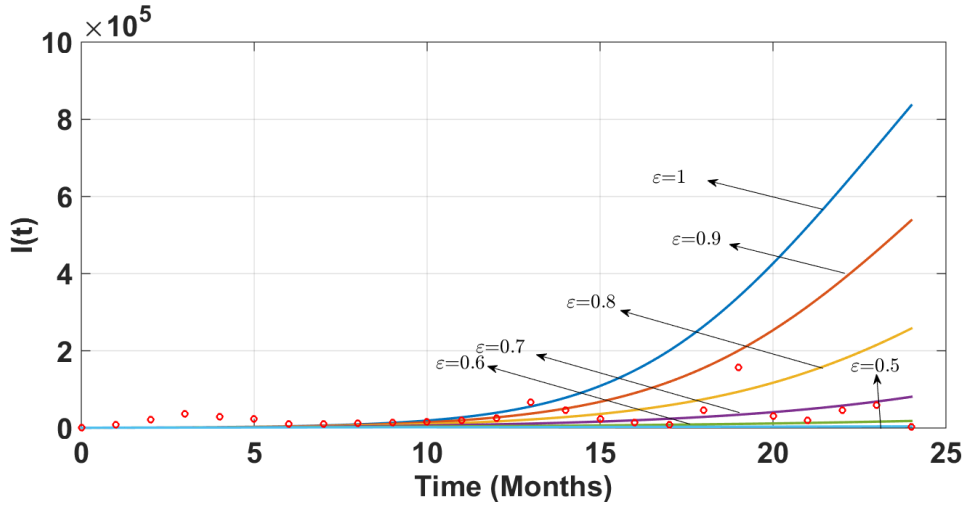

Figure 10: Real data versus model simulation with different values of the fractional-order parameter ε.

“‘

6 Numerical simulations

Since the majority of fractional-order differential equations (FDEs) lack precise analytical solutions, approximation and numerical techniques are required. Different analytical and numerical techniques can be used to solve fractional-order differential equations [60]. In this work, the Adams-Bashforth-Moulton method implemented in Matlab in the routine **fde12** (see [61] and the reference thereien) is used.

For the numerical simulations of our model (13) in COVID-19, some parameters were taken from the literature, but most of them were estimated. Table 2 shows the different parameters with the descriptions and values that allowed us to obtain the curves (Figure 11 and Figures 12).

For Figures 11 and Figures 12, the behavior of the model curves was determined with the initial conditions (S(0)=29977233, E(0) = 370, A(0) = 22027, I(0) = 370, H(0) = 300, R(0)=240). In the simulation, we vary the fractional order ε from 1 to 0.88. We can see from the graphs that fractional order affects the behavior of the curves.

Figure 11 shows the trajectories of the state variables of the fractional order model for exposed individuals E, asymptomatic infectious individuals A, symptomatic infectious individuals I, hospitalized individuals H and recovered individuals R, which tend towards a solution that is the disease-free equilibrium when $\mathcal{R}_0 < 1$. This explains the fact that, in the long term, COVID-19 can disappear from the environment when $\mathcal{R}_0 < 1$. Thus, the behavior of the cured population will increase, which will also affect the susceptible population, and the susceptible population will also gradually increase. The behavior of the state variables is plotted using the parameter values $\beta_h = 0.0868870820652763$ and $\gamma = 0.062703786157422$ and that of Table 2. We obtain $\mathcal{R}_0 = 0.5721$.

With regard to the trajectories of the state variables of our work in Figure 12, we have used the same initial conditions as in Figure 11. The parameter values listed in Table 2 which gives $\mathcal{R}_0 \approx 1.6483$, are used here to illustrate this case. These two parameters allowed us to visualize a behavior different from that in Figure 11. In Figure 12, we observe that the population of exposed E, asymptomatic A, symptomatic I, hospitalized H increases and that the population of susceptible decreases over time, which explains that in the long term COVID-19 will explode in the environment and we will enter an epidemic phase.

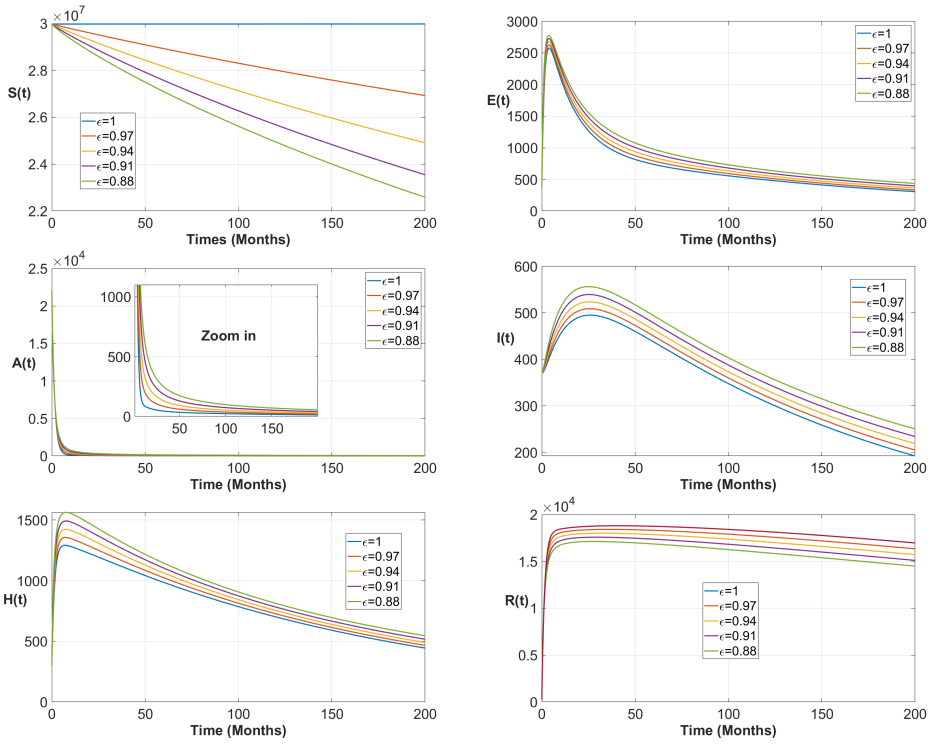

Figure 11: Density graphs of each compartment of the fractional model (13) in the case of DFE.

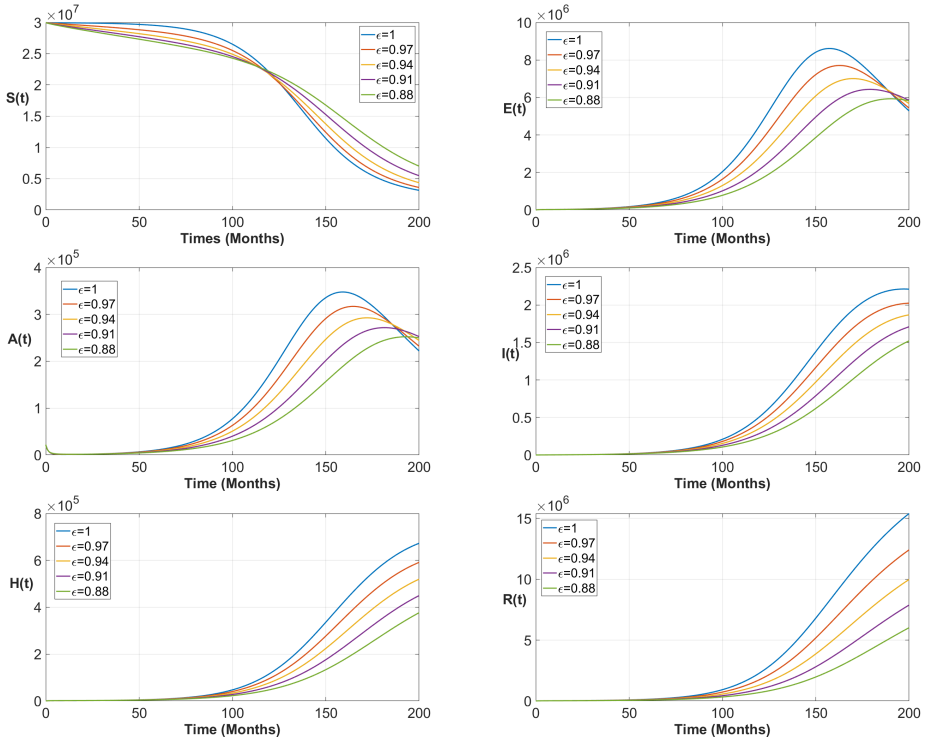

Figure 12: Density graphs of each compartment of the fractional model (13) in the case of the endemic equilibrium.

7 Conclusion and perspectives

In this work, we formulated and investigated a mathematical model of coronavirus transmission dynamics that incorporates the role of the immune system using both classical and fractional derivatives in the Caputo sense.

First, we established the positivity and boundedness of the model solutions. We then proved the existence of equilibrium points and derived the expression of the basic reproduction number $\mathcal{R}_0$ for the classical (integer-order) model. The asymptotic stability of the disease-free equilibrium (DFE) was demonstrated when $\mathcal{R}_0 < 1$, and the existence of an endemic equilibrium was shown for $\mathcal{R}_0 > 1$. Next, we proved the existence and uniqueness of solutions for the fractional-order model. The expression of the basic reproduction number, as well as the existence of equilibrium points and their stability properties, were obtained in the same manner as for the model with classical derivatives.

The model was subsequently calibrated through parameter estimation using real data from Cameroon on confirmed COVID-19 cases recorded between March 2020 and March 2022. With the estimated parameter values, we found that the basic reproduction number is $\mathcal{R}_0 = 1.6483$, indicating that COVID-19 is likely to remain endemic in Cameroon. We also performed a sensitivity analysis of $\mathcal{R}_0$ with respect to the model parameters. The results show that the most influential parameter is the transmission rate (β_h), followed by c_2, which represents the proportion of latent individuals who become symptomatic.

A series of numerical simulations was carried out to visualize the behavior of the fractional-order model and to validate the theoretical results. The simulations indicate that the fractional-order model provides a better fit to the data compared with the classical integer-order model.

The model proposed in this study helps to explain why sub-Saharan African countries have not experienced mortality rates comparable to those observed in developed countries. According to the estimated parameters, the proportion of infected individuals who become susceptible again is higher than the proportion of individuals who effectively contribute to virus transmission within the population.

For future work, we plan to incorporate control strategies into the model in order to assess the concrete impact of intervention measures on reducing new COVID-19 cases in Cameroon. The envisaged control mechanisms include vaccination, barrier measures, social distancing, and the isolation of infected individuals. It is also important to note that this study can be extended to other types of fractional-order derivatives. A major challenge will therefore be to determine, for each fractional-derivative-based model, the value of the fractional-order parameter that best fits the observed data, and subsequently to compare the results obtained.

References

[1] Thirumalaisamy P Velavan and Christian G Meyer. The covid-19 epidemic. *Tropical medicine & international health*, 25(3):278, 2020.

[2] Juan Du, Hong-mei Lang, Yan Ma, Ao-wen Chen, Yong-yi Qin, Xing-ping Zhang, and Chang-quan Huang.

Global trends in covid-19 incidence and case fatality rates (2019–2023): a retrospective analysis. *Frontiers in Public Health*, 12:1355097, 2024.

[3] SÉrvio P Ribeiro, Wesley DÁttilo, David S Barbosa, Wendel Coura-Vital, Igor AS Das Chagas, Camila P Dias, Alcides VC DE Castro E Silva, Maria Helena F Morais, AristÓteles GÓes-Neto, Vasco AC Azevedo, et al. Worldwide covid-19 spreading explained: traveling numbers as a primary driver for the pandemic. *Anais da Academia Brasileira de Ciências*, 92:e20201139, 2020.

[4] Natalia L Komarova, Luis M Schang, and Dominik Wodarz. Patterns of the covid-19 pandemic spread around the world: exponential versus power laws. *Journal of the Royal Society Interface*, 17(170):20200518, 2020.

[5] Henry Loeffler-Wirth, Maria Schmidt, and Hans Binder. Covid-19 transmission trajectories–monitoring the pandemic in the worldwide context. *Viruses*, 12(7):777, 2020.

[6] Elaine Okanyene Nsoesie, Nina Cesare, Martin Müller, and Al Ozonoff. Covid-19 misinformation spread in eight countries: exponential growth modeling study. *Journal of medical Internet research*, 22(12):e24425, 2020.

[7] Adam Ahmat, Sunny C Okoroafor, James Avoka Asamani, Millogo Jean, Abdou Illou Mourtala, Jennifer Nyoni, and Kasonde Mwinga. Health workforce strategies during covid-19 response: insights from 15 countries in the who africa region. *BMC Health Services Research*, 24(1):470, 2024.

[8] Mawada Ali, Salem Mubarak Alzahrani, Rania Saadeh, Mohamed A Abdoon, Ahmad Qazza, Naseam Al-kuleab, and Fathelrhman EL Guma. Modeling covid-19 spread and non-pharmaceutical interventions in south africa: A stochastic approach. *Scientific African*, 24:e02155, 2024.

[9] David Lagoro Kitara and Eric Nzirakaindi Ikoona. Proposed strategies for easing covid-19 lockdown measures in africa. *Pan African Medical Journal*, 36(1), 2020.

[10] Stephanie J Salyer, Justin Maeda, Senga Sembuche, Yenew Kebede, Akhona Tshangela, Mohamed Moussif, Chikwe Ihekweazu, Natalie Mayet, Ebba Abate, Ahmed Ogwell Ouma, et al. The first and second waves of the covid-19 pandemic in africa: a cross-sectional study. *The lancet*, 397(10281):1265–1275, 2021.

[11] Najmul Haider, Abdinasir Yusuf Osman, Audrey Gadzekpo, George O Akipede, Danny Asogun, Rashid Ansumana, Richard John Lessells, Palwasha Khan, Muzamil Mahdi Abdel Hamid, Dorothy Yeboah-Manu, et al. Lockdown measures in response to covid-19 in nine sub-saharan african countries. *BMJ Global health*, 5(10):e003319, 2020.

[12] Rutu Karia, Ishita Gupta, Harshwardhan Khandait, Ashima Yadav, and Anmol Yadav. Covid-19 and its modes of transmission. *SN comprehensive clinical medicine*, 2(10):1798–1801, 2020.

[13] Lei Luo, Dan Liu, Xin-long Liao, Xian-bo Wu, Qin-long Jing, Jia-zhen Zheng, Fang-hua Liu, Shi-gui Yang, Bi Bi, Zhi-hao Li, et al. Modes of contact and risk of transmission in covid-19 among close contacts. *MedRxiv*, pages 2020–03, 2020.

[14] Heshu Sulaiman Rahman, Masrur Sleman Aziz, Ridha Hassan Hussein, Hemn Hassan Othman, Shirwan Hama Salih Omer, Eman Star Khalid, Nusayba Abdulrazaq Abdulrahman, Kawa Amin, and Rasedee Abdullah. The transmission modes and sources of covid-19: A systematic review. *International Journal of Surgery Open*, 26:125–136, 2020.

[15] Esmaeil Mehraeen, Mohammad A Salehi, Farzane Behnezhad, Hamed Rezakhani Moghaddam, and SeyedAhmad SeyedAlinaghi. Transmission modes of covid-19: a systematic review. *Infectious Disorders-Drug TargetsDisorders)*, 21(6):27–34, 2021.

[16] M Altuna, Mª B Sánchez-Saudinós, and Alberto Lleó. Cognitive symptoms after covid-19. *Neurology perspectives*, 1:S16–S24, 2021.

[17] Sonia Villapol. Gastrointestinal symptoms associated with covid-19: impact on the gut microbiome. *Translational Research*, 226:57–69, 2020.

[18] Mun-Keat Looi. How are covid-19 symptoms changing? *bmj*, 380, 2023.

[19] Hatice Rahmet Güner, İmran Hasanoğlu, and Firdevs Aktaş. Covid-19: Prevention and control measures in community. *Turkish Journal of medical sciences*, 50(9):571–577, 2020.

[20] N Deepa, Asmat Parveen, Anjum Khurshid, M Ramachandran, C Sathiyaraj, and C Vimala. A study on issues and preventive measures taken to control covid-19. *AIP Conference Proceedings*, 1(1):1–10, 2022.

[21] Deepak Pradhan, Prativa Biswasroy, Pradeep Kumar Naik, Goutam Ghosh, and Goutam Rath. A review of current interventions for covid-19 prevention. *Archives of medical research*, 51(5):363–374, 2020.

[22] Luigi Cirrincione, Fulvio Plescia, Caterina Ledda, Venerando Rapisarda, Daniela Martorana, Raluca Emilia Moldovan, Kelly Theodoridou, and Emanuele Cannizzaro. Covid-19 pandemic: Prevention and protection measures to be adopted at the workplace. *Sustainability*, 12(9):3603, 2020.

[23] Mohammad Asaduzzaman Chowdhury, Nayem Hossain, Mohammod Abul Kashem, Md Abdus Shahid, and Ashraful Alam. Immune response in covid-19: A review. *Journal of infection and public health*, 13(11): 1619–1629, 2020.

[24] Farzad Taghizadeh-Hesary and Hassan Akbari. The powerful immune system against powerful covid-19: A hypothesis. *Medical hypotheses*, 140:109762, 2020.

[25] Abdurrahman Tufan, Aslihan Avanoğlu Güler, and Marco Matucci-Cerinic. Covid-19, immune system response, hyperinflammation and repurposingantirheumatic drugs. *Turkish journal of medical sciences*, 50(9): 620–632, 2020.

[26] Fereshteh Yazdanpanah, Michael R Hamblin, and Nima Rezaei. The immune system and covid-19: Friend or foe? *Life sciences*, 256:117900, 2020.

[27] Hamadjam Abboubakar, Bruno Buonomo, and Nakul Chitnis. Modelling the effects of malaria infection on mosquito biting behaviour and attractiveness of humans. *Ricerche di matematica*, 65(1):329–346, 2016.

[28] Hamadjam Abboubakar and Racke Reinhard. Mathematical modeling of the coronavirus (covid-19) transmission dynamics using classical and fractional derivatives. *Discrete and Continuous Dynamical Systems - B*, 30(1):289–329, 2025. ISSN 1531-3492. doi: 10.3934/dcdsb.2024089. URL https://www.aimsciences.org/article/id/667d1edbda1208507f7370b0.

[29] Nicolas Bacaër. Ross and malaria (1911). In *A short history of mathematical population dynamics*, pages 65–69. Springer, 2011.

[30] Deccy Y Trejos, Jose C Valverde, and Ezio Venturino. Dynamics of infectious diseases: A review of the main biological aspects and their mathematical translation. *Applied Mathematics & Nonlinear Sciences*, 7(1), 2022.

[31] X Fan, L Wang, and Z Teng. Global dynamics for a class of discrete seirs (susceptible-exposed-infected-recovered-susceptible) epidemic model with general nonlinear incidence. *Adv. Differ. Equ*, 123, 2016.

[32] Duncan K Gathungu, Viona N Ojiambo, Mark EM Kimathi, and Samuel M Mwalili. Modeling the effects of nonpharmaceutical interventions on covid-19 spread in kenya. *Interdisciplinary perspectives on infectious diseases*, 2020(1):6231461, 2020.

[33] Zubair Ahmad, Naveed Khan, Muhammad Arif, Saqib Murtaza, and Ilyas Khan. Dynamics of fractional order sir model with a case study of covid-19 in turkey. *City University International Journal of Computational Analysis*, 4(1):18–35, 2020.

[34] Carlo Delfin S Estadilla, Chiara Cicolani, Rubén Blasco-Aguado, Fernando Saldaña, Alessandro Borri, Javier Mar, Joseba Bidaurrazaga Van-Dierdonck, Oliver Ibarrondo, Nico Stollenwerk, and Maíra Aguiar. The impact of non-pharmaceutical interventions on covid-19 transmission and its effect on life expectancy in two european regions. *BMC Public Health*, 25(1):1004, 2025.

[35] Jaouad Danane, Zakia Hammouch, Karam Allali, Saima Rashid, and Jagdev Singh. A fractional-order model of coronavirus disease 2019 (covid-19) with governmental action and individual reaction. *Mathematical Methods in the Applied Sciences*, 46(7):8275–8288, 2023.

[36] Ihtisham Ul Haq, Nigar Ali, Abdul Bariq, Ali Akgül, Dumitru Baleanu, and Mustafa Bayram. Mathematical modelling of covid-19 outbreak using caputo fractional derivative: stability analysis. *Applied Mathematics in Science and Engineering*, 32(1):2326982, 2024.

[37] Taye Samuel Faniran, Leontine Nkague Nkamba, and Thomas Timothee Manga. Qualitative and quantitative analyses of covid-19 dynamics. *Axioms*, 10(3):210, 2021.

[38] Sadhana Gupta, Yogendra Kumar Rajoria, Govind Prasad Sahu, et al. Mathematical modelling on dynamics of multi-variant sars-cov-2 virus: Estimating delta and omicron variant impact on covid-19. *IAENG International Journal of Applied Mathematics*, 55(1), 2025.

[39] Gauthier Sallet. Mathematical Epidemiology. https://iecl.univ-lorraine.fr/membre-iecl/sallet-gauthier/, March 2018.

[40] Carlos Castillo-Chavez, Sally Blower, Pauline van den Driessche, Denise Kirschner, and Abdul-Aziz Yakubu. *Mathematical approaches for emerging and reemerging infectious diseases: models, methods, and theory*, volume 126. Springer Science & Business Media, 2002.

[41] Pauline Van den Driessche and James Watmough. Reproduction numbers and sub-threshold endemic equilibria for compartmental models of disease transmission. *Mathematical biosciences*, 180(1-2):29–48, 2002.

[42] Zhisheng Shuai and Pauline van den Driessche. Global stability of infectious disease models using lyapunov functions. *SIAM Journal on Applied Mathematics*, 73(4):1513–1532, 2013.

[43] Rubin Fandio, Hamadjam Abboubakar, Henri Paul Ekobena Fouda, Anoop Kumar, and Kottakkaran Sooppy Nisar. Mathematical modelling and projection of buruli ulcer transmission dynamics using classical and fractional derivatives: A case study of cameroon. *Partial Differential Equations in Applied Mathematics*, 8: 100589, 2023.

[44] Joseph P La Salle. *The stability of dynamical systems*. SIAM, 1976.

[45] Santanu Biswas. Assessing the role of active case detection on visceral leishmaniasis control: A case study. *International Journal of Biomathematics*, 17(07):2350065, 2024.

[46] Zaid M Odibat and Nabil T Shawagfeh. Generalized taylor's formula. *Applied Mathematics and computation*, 186(1):286–293, 2007.

[47] I.Podlubny. *Fractional Differential Equations : An Introduction to Fractional Derivatives, Fractional Differential Equations, to Methods of their Solution and some of their Applications*. Elsevier, 1998.

[48] Anatoliĭ Aleksandrovich Kilbas, Hari M Srivastava, and Juan J Trujillo. *Theory and applications of fractional differential equations*, volume 204. elsevier, 2006.

[49] Denis Matignon. Stability results for fractional differential equations with applications to control processing. In *Computational engineering in systems applications*, volume 2, pages 963–968. Lille, France, 1996.

[50] Malik Zaka Ullah, Abdullah K Alzahrani, and Dumitru Baleanu. An efficient numerical technique for a new fractional tuberculosis model with nonsingular derivative operator. *Journal of Taibah University for Science*, 13(1):1147–1157, 2019.

[51] Joseph Yangla, Hamadjam Abboubakar, Ezekiel Dangbe, Richard Yankoulo, Ado Adamou Abba Ari, Irépran Damakoa, and Kottakkaran Sooppy Nisar. Fractional dynamics of a chikungunya transmission model. *Scientific African*, 21:e01812, 2023.

[52] Rubin Fandio, Hamadjam Abboubakar, Banbeto Sylvain Ardo Gouroudja, and Ekobena Fouda Henri Paul. Mathematical modeling of the cholera epidemic in cameroon: From classical-order derivative to fractional-order derivative. *MJ Mathematics and Computer Science*, 1(1):1–32, 2025.

[53] Wei Lin. Global existence theory and chaos control of fractional differential equations. *Journal of Mathematical Analysis and Applications*, 332(1):709–726, 2007.

[54] Ahmed MA El-Sayed. On the existence and stability of positive solution for a nonlinear fractional-order differential equation and some applications. *Alexandria Journal of Mathematics*, 1(1):1–10, 2010.

[55] Adnane Boukhouima, Khalid Hattaf, El Mehdi Lotfi, Marouane Mahrouf, Delfim FM Torres, and Noura Yousfi. Lyapunov functions for fractional-order systems in biology: Methods and applications. *Chaos, Solitons & Fractals*, 140:110224, 2020.

[56] Politologue.com. Evolution du Coronavirus (Covid19) Cameroun. https://coronavirus.politologue.com/coronavirus-cameroun.CM, Accessed: 07-08-2020.

[57] Leontine Nkague Nkamba and Thomas Timothee Manga. Modelling and prediction of the spread of covid-19 in cameroon and assessing the governmental measures (march–september 2020). *COVID*, 1(3):622–644, 2021.

[58] Perspective Monde. Outil pédagogique des grandes tendances mondiales depuis 1945. https://perspective.usherbrooke.ca/bilan/servlet/BMTendanceStatPays/?codeStat=SP.POP.TOTL&codePays=cmr&codeTheme=1, 2025.

[59] N Chitnis, JM Hyman, and JM Cushing. Determining important parameters in the spread of malaria through the sensitivity analysis of a mathematical model. *Bull Math Biol*, 70(5):1272, 2008.

[60] Hao Lu Zhang, Yu Lan Wang, Jun Xi Bi, and Shu Hong Bao. Novel pattern dynamics in a vegetation-water reaction–diffusion model. *Mathematics and Computers in Simulation*, 2025.

[61] Hamadjam Abboubakar, Manasse Djouassoum, Sylvain Ardo Gouroudja Banbeto, and Joseph Yves Effa. Fractional dynamics and prediction of the spread of tuberculosis in the adamaoua region of cameroon. In *Recent Developments in Fractional Calculus: Theory, Applications, and Numerical Simulations*, pages 311–340. Springer, 2025.